Study of the spontaneous nano-emulsification process with different octadecyl succinic anhydride derivatives

Xinyue Wang, Mayeul Collot, Thierry F Vandamme, Nicolas Anton

Study of the spontaneous nano-emulsification process with different octadecyl succinic anhydride derivatives

Xinyue Wang,[a] Mayeul Collot,[b,*] Thierry F. Vandamme,[a,c] Nicolas Anton [a,c,*]

[a] *Université de Strasbourg, CNRS, CAMB UMR 7199, F-67000 Strasbourg, France*

[b] *Université de Strasbourg, CNRS, LBP UMR 7021, F-67000 Strasbourg, France*

[c] *INSERM (French National Institute of Health and Medical Research), UMR 1260, Regenerative Nanomedicine (RNM), FMTS, Université de Strasbourg, F-67000 Strasbourg, France*

* To whom correspondence should be addressed: Nicolas Anton (nanton@unistra.fr) and Mayeul Collot (mayeul.collot@unistra.fr)

Abstract

Three new amphiphilic molecules were synthetized on a basis of a common monomer, octadecyl succinic anhydride (OSA), on which were grafted different PEGylated hydrophilic polar head. The objective of this study is to investigate a potential relationship between the chemical structure of the surfactant, and the efficiency to generate nano-emulsions through the spontaneous nano-emulsification method. Beyond the innovative synthesis and comparison of these amphiphiles, a comprehensive comparison is suggested, comparing size distribution and polydispersity for the different composition parameters, as well making a bridge with critical micelle concentration and hydrophile lipophile balance (HLB). Using OSA monomeric entity as common hydrophobic moiety, the variations in the surfactant molecules were done on the hydrophilic moiety, through the addition of one or two Jeffamine chains in different configurations, so-called $C_{18}^{\ominus}$-PEG, C_{18}-PEG and C_{18}-PEG_2. The results disclosed that $C_{18}^{\ominus}$-PEG allows producing smallest size distribution and lowest PDI values. Moreover, $C_{18}^{\ominus}$-PEG presents the highest critical micellar concentration, linked to a higher hydrophilicity of the molecule. This impacts the balance between surfactant affinity for oil and aqueous phases, a point probably related to the spontaneous emulsification efficiency. A last part of the study regarded the optimization of the emulsification efficiency, through a systematic study in ternary composition map, to disclosed that the best conditions are included in the lower surfactant concentrations, for water and oil contents higher and lower than 50%, respectively. The main idea behind this study was to bring further insights into the unclear relationship between the chemical structure of nonionic surfactants, and the efficiency of the emulsification by spontaneous low-energy method.

1 Introduction

Nano-emulsions (NEs) consist of a colloidal dispersion of two immiscible liquids stabilized by amphiphilic molecules, sizing from around 30 nm to 300 nm [1]. Owning to the high surface area, good physical stability, non-irritant and non-toxicity, and tunable properties, NEs are becoming promising carriers for bioactive compounds and have been extensively investigated in many fields such as drug delivery, diagnostic, cosmetic, pesticide and food industry [2–6].

Comparing with conventional high-energy methods, like high pressure homogenization, ultrasound emulsification, membrane emulsification etc., such low-energy emulsification requires a very limited addition of external energy, but takes advantages of the physico-chemical properties of the compounds to fractionate the oil phase at nano-metric scale. One advantage of this concept lies in the fact that fragile pharmaceutical ingredients are preserved from a potential degradation due to high local energy amount supplied with mechanical homogenization [7]. However, these methods are still not largely used in industry [8], since *(i)* not all surfactants allows an efficient spontaneous emulsification, *(ii)* the physicochemical properties of the NEs dispersion cannot always be finely controlled, in term of size and dispersity, and *(iii)* they involve a significant amount of surfactants, not always compatible with all applications and specifications. Further investigations on the spontaneous emulsification process are then necessary to increase the understanding of the role of surfactant in the process, in order to optimize the applicability of such a low-energy process.

Spontaneous emulsification, or self-emulsification, is performed by gently mixing two liquid phases containing specific surfactants (and/or co-solvents) without any extra energy supply. Spontaneous emulsification was firstly discovered by Johannes Gad in 1879 and has been extensively studied in the last few decades [1,9,10]. Mechanisms behind spontaneous emulsification has been described according to several hypotheses [10,11], originated from interfacial turbulence phenomena, generation of ultralow interfacial tensions, or explained through the solubility changes and sudden migration of the nonionic surfactant in the different phases in presence.

General experimental observations of spontaneous emulsification process give that the main parameters influencing the nano-emulsion size and properties are the compositions and chemical nature of surfactants and oils, temperatures or order of mixing of the different compounds [1,12]. Nevertheless, an universal mechanism has been proposed, based on the respective affinities between surfactants, oils and water phases [1]. The idea proposed a sudden change of the thermodynamic conditions inducing a rapid change of the solubility for surfactant for oil or water, and inducing a turbulence in the system leading to break-up the

oil phase into nano-droplets. This clearly places the surfactant solubility and its temperature sensitivity, as critical for the efficiency of the spontaneous emulsification.

The spontaneous process is related to the sensitivity of the nonionic surfactant (precisely of the poly(ethylene glycol) polar head of the molecule) with the temperature. The most reported examples use commercial surfactant like, *e.g.*, polysorbate (Tween®), sorbitan esters (Span®), polyoxyl 35 castor oil (Kolliphor® EL/ELP) and poloxamer (Pluronic® F68). Upon temperature increasing, these surfactants lose their solubility in water to the benefit of the lipophilic part. As a consequence of the gradual decrease of the number of hydrogen bounding between PEG chain and water molecules, the PEG solubility is reduced. Then, nano-emulsion is generated as a result of a temperature decrease and/or water dilution, resulting from an increase of the solubility of these nonionic surfactants in water [13].

On the other hand, in spite of the number of studies to explain these spontaneous emulsification mechanisms, in spite of the understanding of the impact of the formulation parameters on the size and polydispersity of the nano-emulsion, a part of this concept is still unclear including the relationship between the process efficiency and the chemical nature of both the oil and the surfactants.

The spontaneous emulsification is generally considered to be driven by the affinities between oil and surfactants, impacted by a change of their chemical nature of the former and/or the latter. For instance as regard the impact of the nature of oil, spontaneous emulsification processes reported with castor oil and modified castor oil (tri-iodinated castor oil, in Fig. 2 (b_1) of Ref. [14]), not only shows a significant shift of the nano-emulsion droplet's size of around 100 nm, but also significantly reduces the domain of emulsification process comparing native and modified oil. This observation is recurrent with numerous types of oil phases, an interesting example is the one of *α-tocopherol*, for which the spontaneous emulsification process is not giving nano-scaled droplets —but rather large micrometric droplets— and for which acetate form [15,16] or tri-iodinated form [17,18] is extremely efficient and gives rise to very small (< 50 nm) and very narrow size distribution (PDI < 0.1).

Some reports have emphasized that in the case of spontaneous emulsification where the free energy cost for creating the interfacial area has to be compensated by a large entropic term, thus a flexible surfactant allowing curvature fluctuations is required [19]. Small monomeric surfactants adsorb on the interface of newly form droplets very quickly and result in the production of small droplets, while comparatively polymer generally giving larger droplet size range, *i.e.* inappropriate for the formation of nano-emulsions [20]. Besides the experimental comparison of the results given by nonionic surfactants, comparing each other upon the nano-emulsification process, *predicting* the compatibility of these molecules with spontaneous emulsification process remains, to date, unclear in literature.

In the present study we have synthetized different nonionic surfactants with slight modifications in their chemical structure, and they were compared upon the spontaneous emulsification process. Beside the formulation of NEs, the goal is to understand the impact of the change in the surfactant structure in the efficiency of the process, as well as size and dispersity of the droplet population. The main objective of our investigation here lies in highlighting potential relationship between chemical structure of surfactant and efficiency of emulsification. We have chosen to synthetize octadecyl succinic anhydride derivatives with different functions including grafting of nonionic polymers. It is noteworthy that these new surfactants are not exactly the same as the commercial ones –however very close in the chemical structure principle– but our idea was to get a series of molecules very close each other only differing in one chemical function, to compare them as regards the emulsification efficiency.

2 Materials and methods

2.1 Materials

Octadecyl succinic anhydride (OSA) and vitamin E acetate (VEA) were purchased from Tokyo Chemical Industry. Polyetheramine Jeffamine® M-2070 (J-2000) was kindly offered by Huntsman Corporation. Ethanol, ethanolamine, triethylamine (TEA), dimethylformamide (DMF), dichloroform (DCM) and hexafluorophosphate azabenzotriazole tetramethyl uranium (HATU) were obtained from Merck-Millipore. Phosphate buffered saline (PBS) was from Eurobio (Courtaboeuf, France).

2.2 Synthesis

The structures of three amphiphilic molecules specially synthetized for this study, so-called**$C_{18}^{\ominus}$-PEG** , **C_{18}-PEG** and **C_{18}-PEG$_2$** , are illustrated in Fig. 1, and the synthesis procedures are described below. These surfactants arise from the reaction of the amine (NH_2) terminated PEG (J-2000) on amine-reactive anhydride (OSA) first providing **$C_{18}^{\ominus}$-PEG**, which thus bears a carboxylic acid function. This function was then either reacted with another J-2000 (forming **C_{18}-PEG$_2$**), or capped with ethanolamine (forming **C_{18}-PEG**).

$C_{18}^{\ominus}$-PEG: To a solution of OSA (352 mg, 1 mmol) in DMF (20 mL) was added J-2000 (2 g, 1 mmol) dissolved in DMF (10 mL). After the homogeneity, 696 µL of TEA (5 mmol, 5 eq) were added to the solution following a heating up to 60°C overnight. Then, the solvent was evaporated. For the purification, firstly, the crude was dissolved in DCM, and then washed

three times by 1 M HCl in saturated NaCl solution. The organic phase was dried over anhydrous sodium sulfate, filtrated over cotton and evaporated.

C_{18}-PEG$_2$: To a solution of OSA (352 mg, 1 mmol) in DMF (20 mL) was added J-2000 (4 g, 2 mmol, 2 eq) dissolved in DMF (20 mL). After the homogeneity, 696 µL of TEA (5 eq) and HATU (570 mg, 1.5 eq) were added to the solution following a heating up to 60°C overnight. Then, the solvent was evaporated. For the purification, firstly, the crude was dissolved in ethanol, and then dialysis was conducted with a regenerated cellulose membrane (molecular weight cutting off is 2,000 Da). Outside media (ethanol) was changed every 8 h for 3 times. The final product was obtained with evaporation of ethanol.

C_{18}-PEG: To a solution of OSA (352 mg, 1 mmol) in DMF (20 mL) was added J-2000 (2 g, 2 mmol, 2 eq) dissolved in DMF (10 mL). After the homogeneity, 696 µL of TEA (5 eq) was added to the solution following a heating up to 60°C overnight. Then, 60 µL of ethanolamine (1 eq dissolved in 5 mL DMF) and HATU (570 mg, 1.5 eq) were added to the solution at the same temperature overnight again. Next, the solvents were evaporated, and the purification was strictly the same as described for **C_{18}-PEG$_2$**.

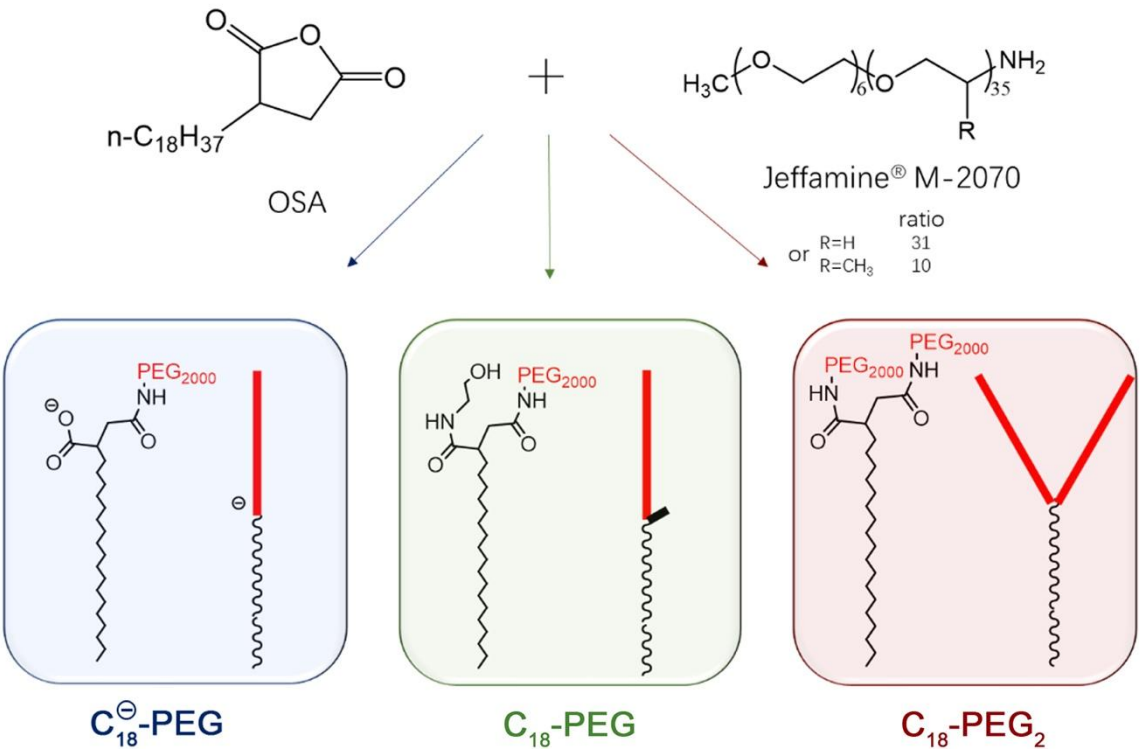

Figure 1: Synthesis and structure scheme of the three amphiphilic molecules synthetized. Red chain symbolizes the PEG chains.

2.3 Structure confirmation

To confirm the structure of three molecules, around 40 mg of products were dissolved in 500 µL $CDCl_3$ for NMR tests. Both ^{1}H-NMR and ^{13}C-NMR spectra were recorded on a Bruker Avance III 400 MHz spectrometer.

2.4 Critical micelle concentration (CMC) determination

The CMC of three amphiphilic molecules were determined by a fluorescence method using Nile red (NR) as a probe [21]. NR in DMSO (200 µM) was used as a stock solution. Firstly, a series of 1 mL solutions of each surfactant (with concentrations ranging from 0.001 to 10 mg/mL) in milliQ water were prepared, and 5 µL of NR stock solution were added into each sample to reach a final NR concentration of 1µM. Fluorescence spectra were recorded at 20°C at a fixed excitation of 530 nm, and the emission was monitored from 540 nm to 800 nm. The maximum emission wavelength (λ_{em}) was recorded and presented for the CMC calculation, corresponding to the intercept between the straight baseline (before CMC) and the rising straight line of the fluorescence signal (after CMC).

2.5 hydrophile lipophile balance (HLB) calculation

HLB values of each amphiphilic molecule were calculated according to the commonly used Davies' group contribution method [22]. Details of the equation and table of parameters are reported in the *Supplementary information* section, Eq. S1 and Table S1, respectively.

2.6 Emulsification

Spontaneous emulsification method was used as reported in previous papers [16,23]. In brief, surfactants were dissolved in oil phase with different *surfactant to oil weight ratio* (SOR) at a set temperature, then PBS, maintained at the same temperature, was added according to different *(surfactant + oil) to water weight ratio* (SOWR). After vortex homogenization for 1 min, following a mixing in a thermomixer at 2,000 rpm for 10 min nano-emulsions were formed. In order to explore and optimize the emulsification conditions, the process was performed at different compositions and environmental conditions.

Size distribution, polydispersity index and ξ potential were determined by dynamic light scattering (DLS) with NanoZS (Malvern, Orsay, France). Generated emulsions were diluted by 100 and 1,000 times in distilled water, for size and ξ potential measurements, respectively.

3 Results and discussion

3.1 Structure identification of new molecules

Due to the simple synthesis process, the reaction yield for each molecule was above 90%. Structures of the three amphiphilic molecules are shown in Fig. 1. With the similar hydrophobic saturated aliphatic chain (shown in black), the difference in these molecules arose in their hydrophilic head (red). Three different variations (see Fig. 1) of their polar head compositions came from the fact that **$C_{18}^{\ominus}$-PEG** beared a -COOH, potentially becoming carboxylate when solvated at the oil/water interface and in PBS (pH 7.4), while for **C_{18}-PEG**, the capped ethanolamine part annihilated the charge, and for the **C_{18}-PEG$_2$** the carboxylic acid was replaced by another J-2000. The structures were unambiguously identified by ^{1}H and ^{13}C NMR spectra (the identical parts shown in Fig. 2, while the complete spectra were reported in the *Supplementary information* section). It followed that, as **$C_{18}^{\ominus}$-PEG** and **C_{18}-PEG** are shown to bear two different amide moieties (carbon 1 and 4 shown in Fig. 2A), two different carbonyl signals could be observed in ^{13}C NMR (δ 179.83 and 176.78 ppm for **$C_{18}^{\ominus}$-PEG**, 176.53 and 173.17 ppm for **C_{18}-PEG**). On the contratry, **C_{18}-PEG$_2$** only showed one carbonyl signal at 174.27 ppm due to the similarity of the amide moiteies (Fig. 2B). In addition, in Fig. 2C, integration of the number of protons (^{1}H NMR) of the PEG moieties appeared consistent with their supposed structure: proton intergrations at ~1.1 ppm (peaks c) and ~3.6 ppm (peaks d and e) appeared twice higher for **C_{18}-PEG$_2$**, which have two PEG chains, compared to **$C_{18}^{\ominus}$-PEG** and **C_{18}-PEG** having one PEG chain.

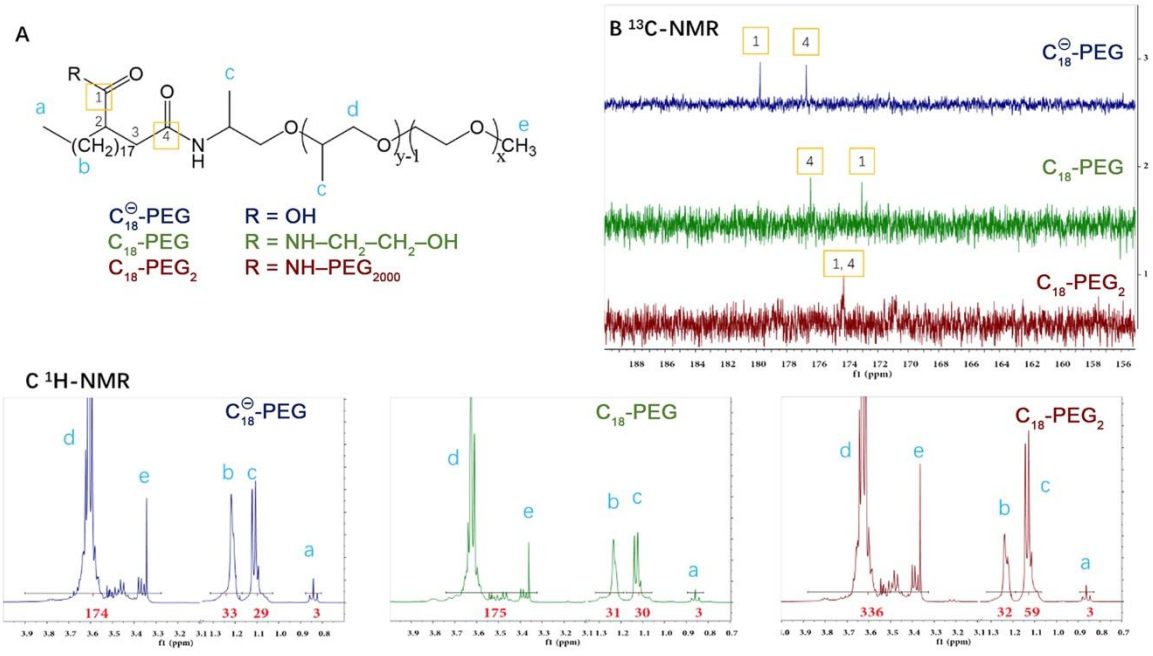

Figure 2: NMR spectra of three synthesized surfactants.

3.2 Physico-chemical characterization of the surfactants

Physicochemical properties of surfactants are crucial to understand their behavior and potential applications, along with the fact that they play a critical role on structure-activity relationship screening. Beside appearance and molecular weight, CMC and HLB were determined, allowing a first comparison. Results concerning the determination of CMC are reported in Fig. 3 and all data summarized in table 1 (see details regarding the fluorescent spectra are reported in Fig. S1, in the *Supplementary Information* section). HLB values were rather comparable between **$C_{18}^{\ominus}$-PEG**, **C_{18}-PEG** (12.3 and 14.3, respectively), but increased up to 22.8 for **C_{18}-PEG_2** respectively. All these surfactants had a HLB value significantly high, enough to be considered as very hydrophilic, compatible with application as stabilizer for direct emulsification. Interestingly, the HLB value of **C_{18}-PEG_2** jumped to 22.8, significantly higher than the two formers. As regards the CMC values, a significant gap appeared between the neutral (**C_{18}-PEG** and **C_{18}-PEG_2** around 0.02 g/L) and charged surfactants (**$C_{18}^{\ominus}$-PEG** around 0.036 g/L), reflecting the higher solubility of the molecule coming from its ionic nature. Indeed, the higher the water solubility, the higher the CMC, as described in literature [24]. As a last remark, the comparison of the CMC and HLB values were not exactly inline each other, likely explained by the fact that HLB remained calculations based on chemical structure, whereas CMC determination was based on the actual experimental behavior. Nevertheless, HLB values of all these surfactants indicated they are very hydrophilic molecules.

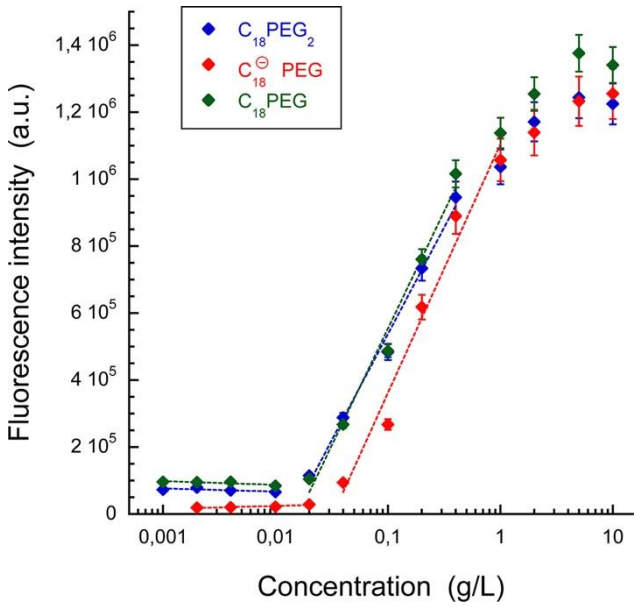

Figure 3: Determination of the Critical Micelle Concentration of the different amphiphile molecules, using Nile Red as fluorescent probe (see details in the text, *section 2.4*).

Table 1: Physicochemical properties of three new surfactants

Product	Appearance (R.T.)	M.W.	CMC (20°C)	HLB
$C_{18}^{\ominus}$-PEG	white-yellowish paste	~2300	0.036 mg/ml	12.3
C_{18}-PEG	white-yellowish wax	~2350	0.021 mg/ml	14.3
C_{18}-PEG_2	yellow wax	~4300	0.018 mg/ml	22.8

3.3 Emulsification efficiency of three surfactants

Although spontaneous emulsification provided a much convenient and economic method for nano-emulsification, the formulation was not as predictable as the mechanical methods. The general route to study spontaneous emulsification process was generally done [1] following-up of the size distribution of the nano-emulsions along with modifications of compositions parameters like surfactant amount (with SOR), dispersed volume fraction (with SOWR), or environment parameters like, *e.g.*, temperature. These key parameters were investigated for that purpose, with the idea to disclose the structure-properties relationship.

3.3.1 Effect of surfactant concentration

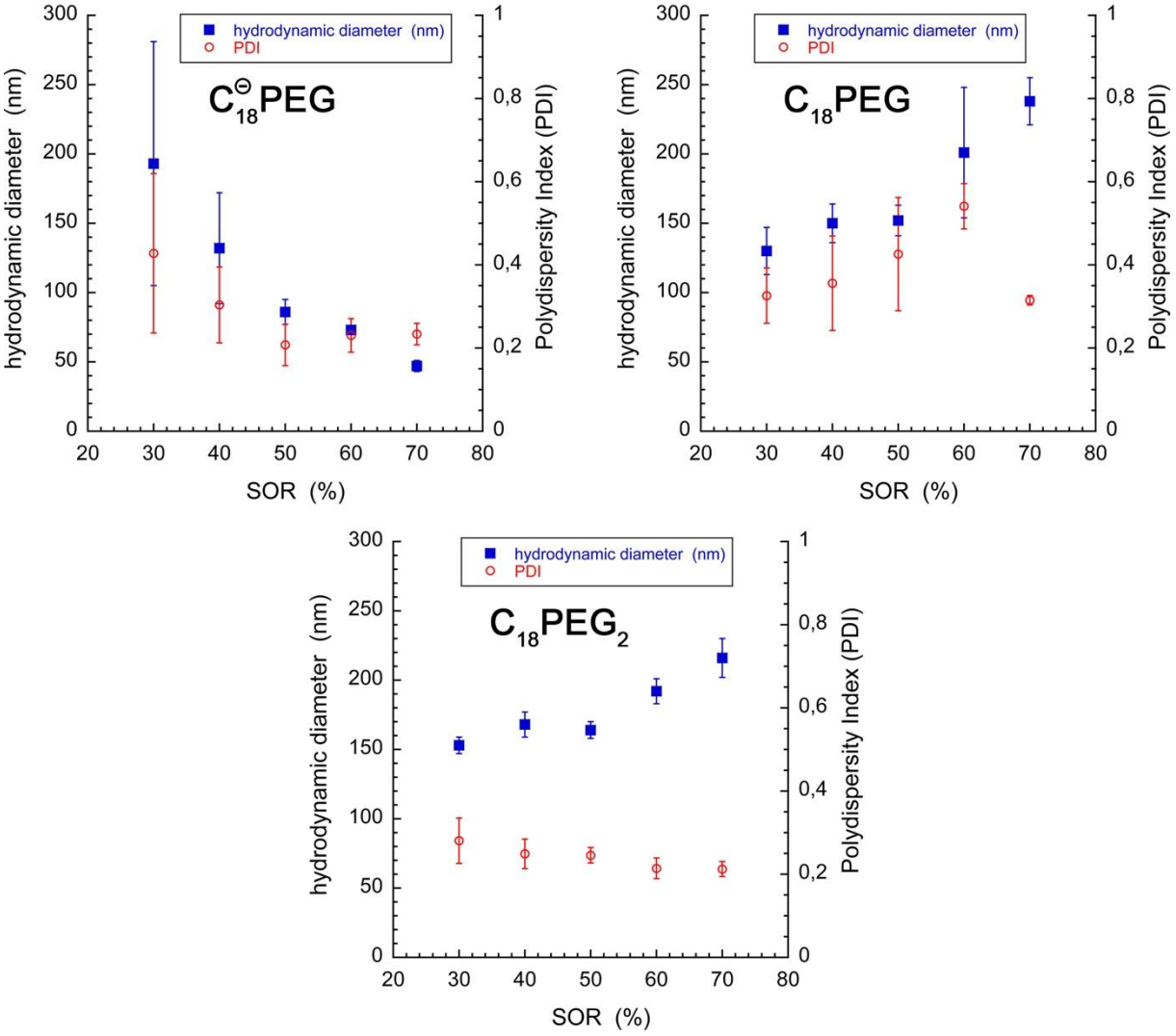

Figure 4: Size and PDI of NEs prepared using $C_{18}^{\ominus}$-PEG, C_{18}-PEG and C_{18}-PEG_2, in function of the values of SOR, at constant SOWR = 5% and at emulsification temperature T = 90°C.

For this first series of experiments, the SOR (linked to surfactant amount) was gradually increased and the size distribution (*i.e.* average diameter and polydispersity indexes (PDI)) was measured. Thus, SORs varied from 30% to 70%, at a fixed SOWR of 5% and a fixed temperature of the emulsification process of 90°C, temperature at which both the {oil + surfactant} and the water phases were maintained before mixing. Results were reported in Fig. 4. The case of **$C_{18}^{\ominus}$-PEG** (Fig. 4A) showed the most conventional behavior compared to literature [1,25], where increasing the SOR value induced a decrease in the mean droplet's size and PDI. Reproducibility was improved with SOR. It is important to note that nano-emulsions were considered monodispersed, and therefore the spontaneous process considered as efficient, when the PDI was lower than 0.25; in that case, this criterion was met for SOR > 50%, when the droplet size decreased below 90 nm. This trend was generally

attributed to the increasing efficiency of surfactant at the interface, related to the interfacial concentration as the bulk concentration was increased.

On the other hand, in Fig. 4B and Fig. 4C, for **C_{18}-PEG** and **C_{18}-PEG_2**, respectively, an opposite trend arose, showing an increase of the droplet size with the SOR. These results clearly contrasted with the ones generally obtained [1,14,17,26] with such processes, since, unlike **$C_{18}^{\ominus}$-PEG**, in that cases the droplet size and PDI increased with increasing surfactants amount. In addition, in the case of **C_{18}-PEG,** the PDI values are too high (> 0.25) for validating the measurements, while they conserved a good value (< 0.25) in the case of **C_{18}-PEG_2**. In both cases, emulsification process seemed to be affected by these chemical modifications. The lower CMC disclosed in Fig. 3 for **C_{18}-PEG** and **C_{18}-PEG_2** might be related to this behavior, indicating that a lower water solubility affected the interfacial behavior at high concentrations. It is interesting to note, as well, that the process of droplet coalescence after emulsification could be slowed down by their surface charge, orienting the global size distribution towards smaller size range with charged molecules, as observed. This was confirmed with the values of zeta potential, measured at -28 mV and -30.0 mV for **C_{18}-PEG** and **C_{18}-PEG_2**, respectively, when it raised at -39 mV for the charged **$C_{18}^{\ominus}$-PEG** surfactant.

3.3.2 Effect of water ratio

The effect of water concentration was investigated by preparing a series of emulsions with different SOWRs from 2% to 20%, at a fixed SOR of 50% and a fixed emulsification temperature of 90°C. The results, reported in Fig. 5, overall showed a decrease and stabilization of the size as the water content increased. In general, the impact of the water ratio was considered as not impacting on the nano-emulsion size, and this is effectively observed with SOWR ≥ 5%. On the other hand, for very high proportions of water (low SOWRs) the quality of the emulsion was surprisingly decreased and size increased. This feature was probably not documented since such concentration range had a limited interest. However, it reveals that a minimum volume fraction of dispersed phase was required in order to make efficient the spontaneous emulsification process.

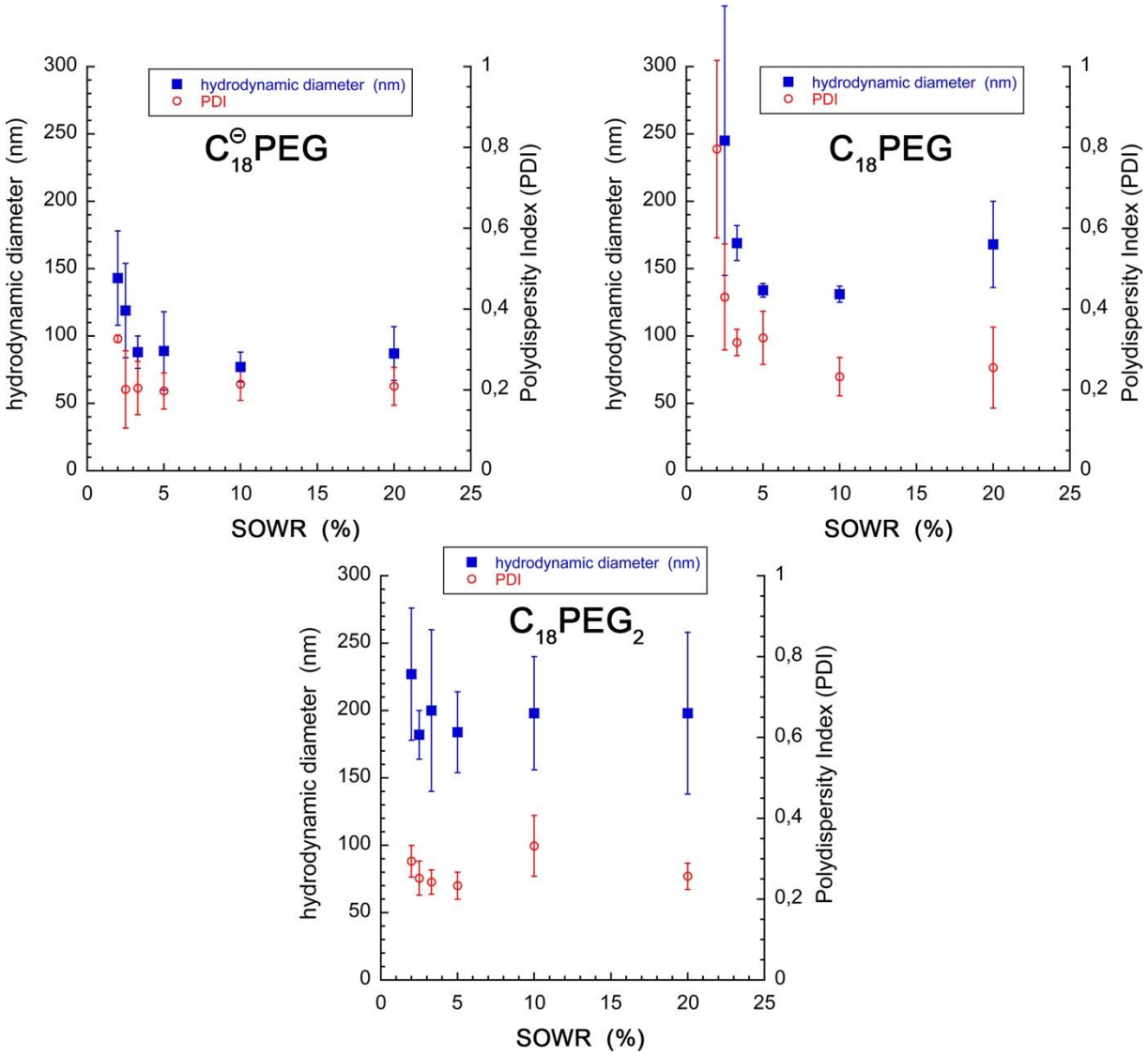

Figure 5: Size and PDI of NEs prepared using $C_{18}^{\ominus}$-PEG, C_{18}-PEG and C_{18}-PEG_2, in function of the values of SOWR, at constant SOR = 50% and at emulsification temperature T = 90°C.

3.3.3 Effect of emulsification temperature

Spontaneous nano-emulsification process was based on the physico-chemical behavior of nonionic surfactants, and particularly on their temperature sensitivity [13]. Indeed, playing on temperature modified the solubility of the PEG chains and, in certain conditions, induced the spontaneous generation of droplets. In previous reported studies [1,13,27], we described the impact of the emulsification temperature on the process itself, giving the temperature threshold impacting on the process efficiency. Indeed, if the emulsification temperature was below the cloud point –or phase inversion temperature– the process dramatically lose efficiency below those temperature thresholds. In the present case of comparison, different surfactants, investigating this parameter appeared important to understand their impact on the emulsification process. To this end, emulsions were prepared from 60°C to 90 °C with a

fixed SOR of 50% and SOWR of 5%. Results are shown in Fig. 6. This parameter had a significant impact on the nano-emulsions' properties. Considering **$C_{18}^{\ominus}$-PEG**, for T < 80°C, the size, PDI and reproducibility was clearly affected, when compared to T ≥ 80°C where these parameters were much better and reproducible. This result confirmed the thermo-sensitivity and the behavior expected for such nonionic surfactants. On the other hand, this conclusion could not be drawn for the other surfactants (**C_{18}-PEG** and **C_{18}-PEG_2**), for which the temperature did not seem to have a real impact on the process efficiency. For these surfactants, in those conditions (SOR and SOWR values), the PDI values remained quite high, and we could conclude that the nano-emulsions generated did not meet quality criteria. It can be explained by the surfactant's affinities for aqueous and oil phase, not optimally balanced for inducing sufficient turbulences during the emulsification. Another factor that could induce the un-robustness of such processes, was the oil phase viscosity transitory which significantly varied with the temperature. Indeed, from 60°C to 90 °C, VEA viscosity decreased almost four times [28], which could impact on the properties of droplets fractionation.

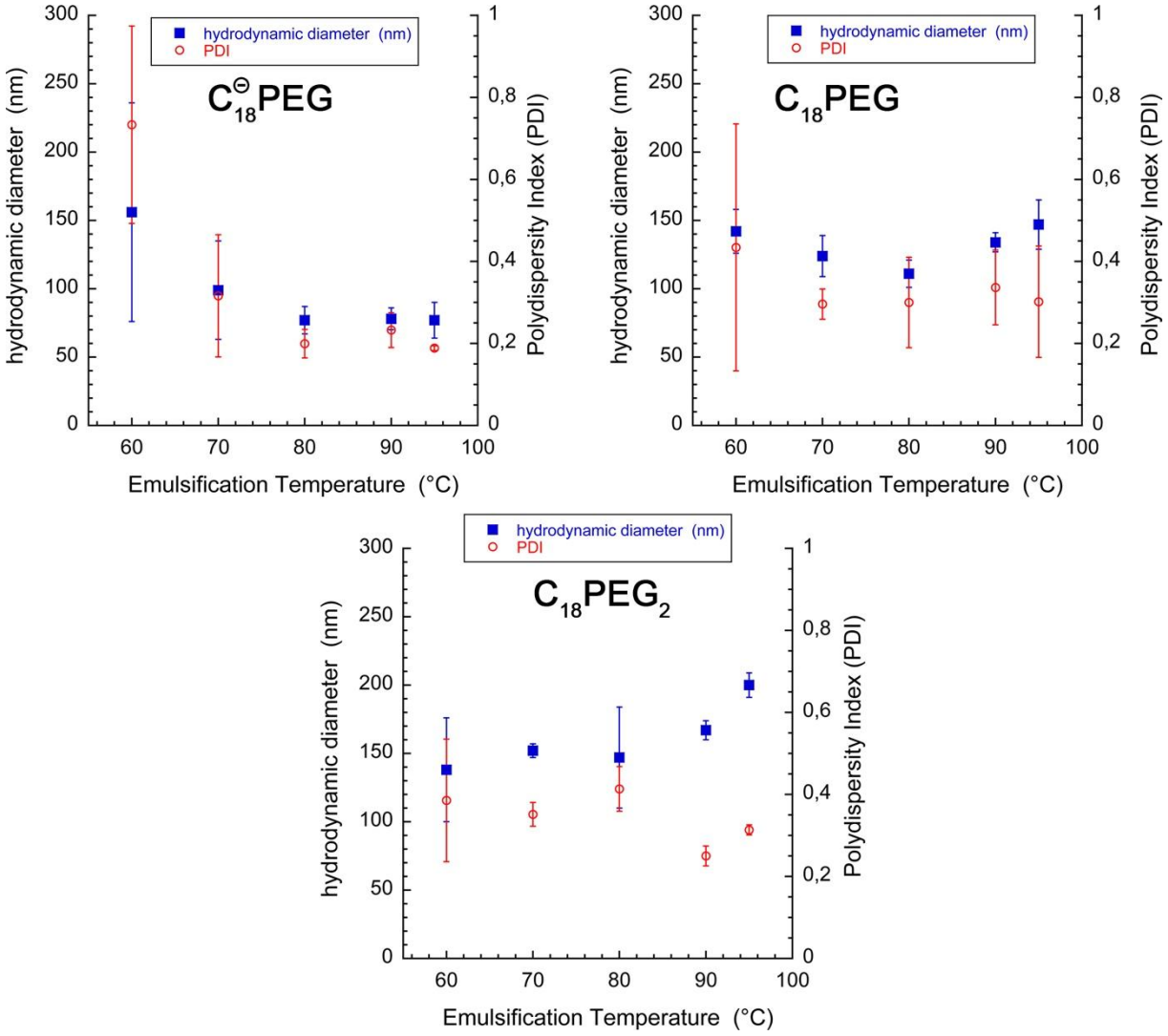

Figure 6: Size and PDI of NEs prepared using $C_{18}^{\ominus}$-PEG, C_{18}-PEG and C_{18}-PEG_2, in function of the values of emulsification temperature, at constant SOR = 50% and SOWR = 5%.

3.4 Optimization of nano-emulsification process

To gain further insights into the spontaneous emulsification process obtained with these new surfactants, a screening of formulations (38 different formulations, see Fig. 7 (A)) was undertaken and compared each other. This part focused on the **$C_{18}^{\ominus}$-PEG**, that showed the best nano-emulsions, and allowed comparing finely the impact of the composition on the emulsification process. The corresponding results, as size distribution and PDI, are shown in Fig. 7 (B) and (C), respectively. In Fig. 7 (B), the red line delimited the region where emulsions are sizing below 250 nm, thus, so-called *nano-emulsions*. The small zones indicated with deepen blue showed sizes below 25 nm, possibly small nano-emulsions, but could also be swollen micelles (micelles swollen by oil [27]). The main results given by Fig. 7 (B) are *(i)* nano-emulsions feasibility domain overall corresponded to low oil ratio, below 25%. Increasing of oil quantity resulted in the lack of surfactant coverage of the oil-water interface; *(ii)* On the other hand, an excess of surfactant (with reduction of water), formed a

concentrated surfactant phase containing high amount of micelles, and for the most concentrated regions, turned into *gel phase* probably forming liquid crystalline phases [29,30]. In Fig. 7 (C), the red line emphasized the region of PDI values lower than 0.3, for which we considered the population monodisperse and stable. In Fig. 7 (D), the focus was done on the water corner of Fig. 7 (B), showing the nano-emulsification in the more diluted conditions, up to SOWR equal to 20 %. Red and green arrows indicated the increase of SOR and SOWR, respectively. Such region corresponds to the emulsification studied above and confirmed that nano-emulsification process is mainly driven by surfactant amount, with a weak influence of the other formulation parameters.

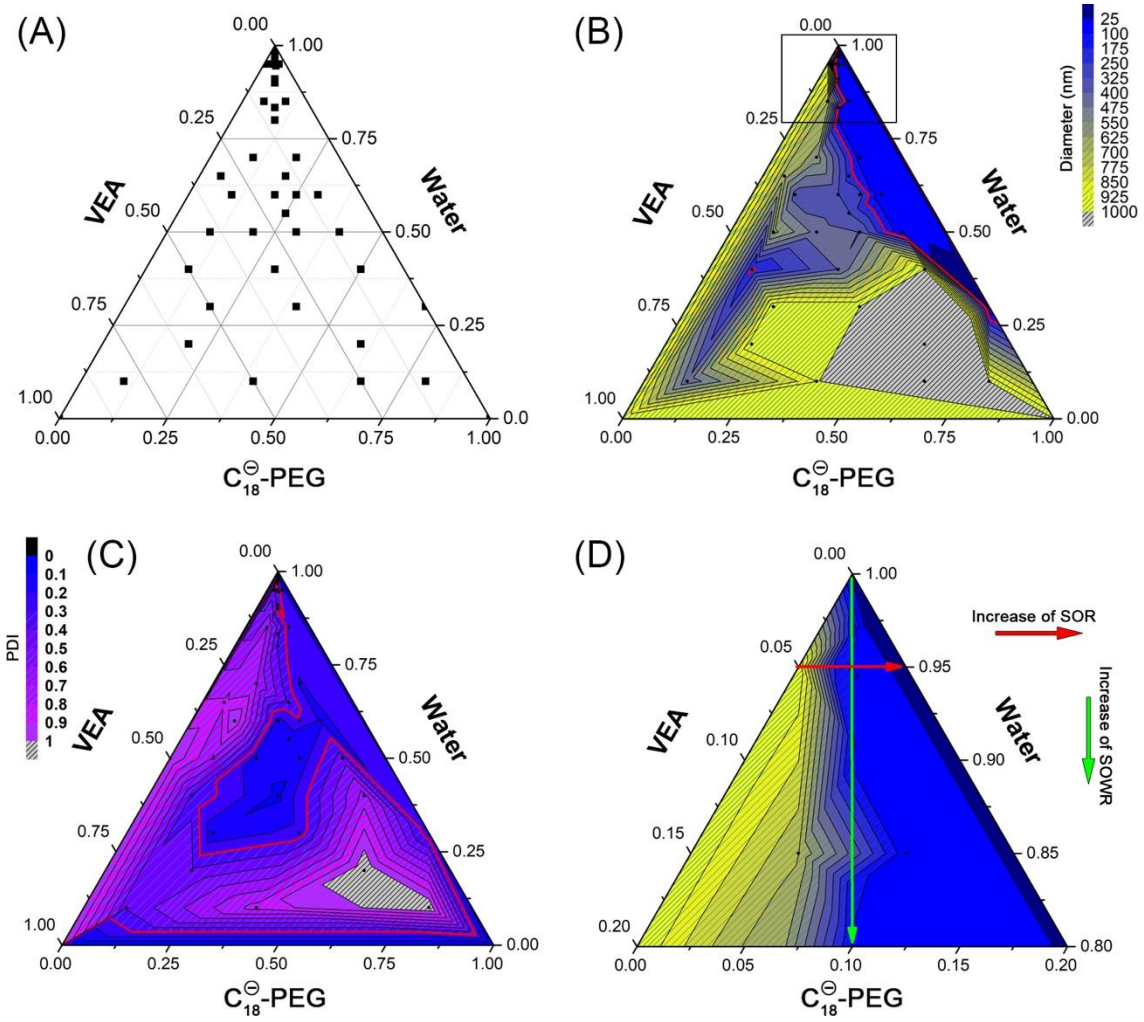

Figure 7 Investigation of the composition on the emulsification of **$C_{18}^{\ominus}$-PEG**, with the ternary system composed of **$C_{18}^{\ominus}$-PEG** (surfactant), oil (VEA vitamin E acetate) and water. (A) Screening of the formulations studied, (B) Values of the mean size of the droplet population (hydrodynamic diameter). (C) PDI values corresponding to the results reported in part (B). (D) Focus on the water corner of part (B), indicated with a square.

In this study, we mainly focused the investigation on the potentials offered by OSA derivatives. OSA readily led to amphiphilic molecules which could easily be modified as

derivatives with modulated properties that showed the potential to act as an emulsifier. It is noteworthy that such approaches have been approved by the FDA for use in food industry, for example in the case of OSA starches used as emulsifiers and encapsulating agents which can form emulsions with an average size around 500 µm [31]. In addition, one advantage of these derivative owed to their independency of ionic strength [32].

4 Conclusion

In this study, we synthetized new amphiphilic molecules and studied their ability for generating emulsions and nano-emulsions by spontaneous emulsification method. Based on a common basis of OSA as monomeric entity, the variations in the surfactant molecules were done on the hydrophilic moiety, through the addition of one or two Jeffamine chains in different configurations, so-called **$C_{18}^{\ominus}$-PEG**, **C_{18}-PEG** and **C_{18}-PEG_2**. This study not only shows the simplicity of the chemical modification of OSA, but also the significant impact on the spontaneous process and properties of the droplet population. The comparison of these three surfactants, gave that **$C_{18}^{\ominus}$-PEG** performed the smallest size distribution and lowest PDI values. From the structure-activity point of view, HLB values are globally calculated in comparable range, whereas regarding the CMC, **$C_{18}^{\ominus}$-PEG** appears more hydrophilic compared to **C_{18}-PEG** and **C_{18}-PEG_2**, very close each other. As the spontaneous emulsification process is related to the balance between surfactant affinity for oil and aqueous phases, this point could explain the slight difference between process efficiency revealed. From an optimization experiment, we disclosed that the best conditions are included in the lower surfactant concentrations, for water and oil contents higher and lower than 50%, respectively. Among all the factors impacting on the spontaneous emulsification, a larger SOR and a higher emulsification temperature could benefit the fabrication, while SOWR had limited influence.

5 Acknowledgements

The authors thank the China Scholarship Council for funding Ph.D. fellowship for X.W., (CSC No. 201706240033).

6 References

[1] N. Anton, T.F. Vandamme, The universality of low-energy nano-emulsification, Int. J. Pharm. 377 (2009) 142–147.

https://doi.org/https://doi.org/10.1016/j.ijpharm.2009.05.014.

[2] X. Li, N. Anton, G. Zuber, T. Vandamme, Contrast agents for preclinical targeted X-ray imaging, Adv. Drug Deliv. Rev. 76 (2014) 116–133. https://doi.org/10.1016/j.addr.2014.07.013.

[3] Y. Singh, J.G. Meher, K. Raval, F.A. Khan, M. Chaurasia, N.K. Jain, M.K. Chourasia, Nanoemulsion: Concepts, development and applications in drug delivery, J. Control. Release. 252 (2017) 28–49. https://doi.org/https://doi.org/10.1016/j.jconrel.2017.03.008.

[4] O. Sonneville-Aubrun, M.N. Yukuyama, A. Pizzino, Chapter 14 - Application of Nanoemulsions in Cosmetics, in: S.M. Jafari, D.J. McClements (Eds.), Nanoemulsions, Academic Press, 2018: pp. 435–475. https://doi.org/https://doi.org/10.1016/B978-0-12-811838-2.00014-X.

[5] L. Wang, X. Li, G. Zhang, J. Dong, J. Eastoe, Oil-in-water nanoemulsions for pesticide formulations, J. Colloid Interface Sci. 314 (2007) 230–235. https://doi.org/https://doi.org/10.1016/j.jcis.2007.04.079.

[6] D.J. McClements, J. Rao, Food-Grade Nanoemulsions: Formulation, Fabrication, Properties, Performance, Biological Fate, and Potential Toxicity, Crit. Rev. Food Sci. Nutr. 51 (2011) 285–330. https://doi.org/10.1080/10408398.2011.559558.

[7] R. Bouchaala, L. Mercier, B. Andreiuk, Y. Mély, T. Vandamme, N. Anton, J.G. Goetz, A.S. Klymchenko, Integrity of lipid nanocarriers in bloodstream and tumor quantified by near-infrared ratiometric FRET imaging in living mice, J. Control. Release. 236 (2016). https://doi.org/10.1016/j.jconrel.2016.06.027.

[8] N. Anton, T.F. Vandamme, Nano-Emulsions, in: M. Aliofkhazraei (Ed.), Handb. Nanoparticles, Springer International Publishing, Cham, 2016: pp. 93–116. https://doi.org/10.1007/978-3-319-15338-4_2.

[9] Z. Li, D. Xu, Y. Yuan, H. Wu, J. Hou, W. Kang, B. Bai, Advances of spontaneous emulsification and its important applications in enhanced oil recovery process, Adv. Colloid Interface Sci. 277 (2020) 102119. https://doi.org/https://doi.org/10.1016/j.cis.2020.102119.

[10] C. Solans, D. Morales, M. Homs, Spontaneous emulsification, Curr. Opin. Colloid Interface Sci. 22 (2016) 88–93. https://doi.org/https://doi.org/10.1016/j.cocis.2016.03.002.

[11] J.C. López-Montilla, P.E. Herrera-Morales, S. Pandey, D.O. Shah, Spontaneous Emulsification: Mechanisms, Physicochemical Aspects, Modeling, and Applications, J. Dispers. Sci. Technol. 23 (2002) 219–268. https://doi.org/10.1080/01932690208984202.

[12] A. Gupta, Z. Badruddoza, P.S. Doyle, A General Route for Nanoemulsion Synthesis using Low Energy Methods at Constant Temperature, Langmuir. 33 (2017) 7118–7123. https://doi.org/10.1021/acs.langmuir.7b01104.

[13] N. Anton, S. Akram, T.F. Vandamme, Chapter 4 - Transitional Nanoemulsification Methods, in: S.M. Jafari, D.J. McClements (Eds.), Nanoemulsions, Academic Press,

2018: pp. 77–100. https://doi.org/https://doi.org/10.1016/B978-0-12-811838-2.00004-7.

[14] M.F. Attia, N. Anton, M. Chiper, R. Akasov, H. Anton, N. Messaddeq, S. Fournel, A.S. Klymchenko, Y. Mély, T.F. Vandamme, Biodistribution of X-ray iodinated contrast agent in nano-emulsions is controlled by the chemical nature of the oily core, ACS Nano. 8 (2014) 10537–10550. https://doi.org/10.1021/nn503973z.

[15] X. Li, N. Anton, T.M. Ta, M. Zhao, N. Messaddeq, T.F. Vandamme, Microencapsulation of nanoemulsions: novel Trojan particles for bioactive lipid molecule delivery., Int. J. Nanomedicine. 6 (2011).

[16] X. Wang, N. Anton, P. Ashokkumar, H. Anton, T.K. Fam, T. Vandamme, A.S. Klymchenko, M. Collot, Optimizing the Fluorescence Properties of Nanoemulsions for Single Particle Tracking in Live Cells., ACS Appl. Mater. Interfaces. 11 (2019) 13079–13090. https://doi.org/10.1021/acsami.8b22297.

[17] X. Li, N. Anton, G. Zuber, M. Zhao, N. Messaddeq, F. Hallouard, H. Fessi, T.F. Vandamme, Iodinated α-tocopherol nano-emulsions as non-toxic contrast agents for preclinical X-ray imaging, Biomaterials. 34 (2013) 481–491. https://doi.org/10.1016/j.biomaterials.2012.09.026.

[18] N. Anton, A. Parlog, G. Bou About, M.F. Attia, M. Wattenhofer-Donzé, H. Jacobs, I. Goncalves, E. Robinet, T. Sorg, T.F. Vandamme, Non-invasive quantitative imaging of hepatocellular carcinoma growth in mice by micro-CT using liver-targeted iodinated nano-emulsions, Sci. Rep. 7 (2017). https://doi.org/10.1038/s41598-017-14270-7.

[19] Y. Chevalier, New surfactants: new chemical functions and molecular architectures, Curr. Opin. Colloid Interface Sci. 7 (2002) 3–11. https://doi.org/https://doi.org/10.1016/S1359-0294(02)00006-7.

[20] E. Bouyer, G. Mekhloufi, V. Rosilio, J.-L. Grossiord, F. Agnely, Proteins, polysaccharides, and their complexes used as stabilizers for emulsions: Alternatives to synthetic surfactants in the pharmaceutical field?, Int. J. Pharm. 436 (2012) 359–378. https://doi.org/https://doi.org/10.1016/j.ijpharm.2012.06.052.

[21] Y. Xia, H. He, X. Liu, D. Hu, L. Yin, Y. Lu, W. Xu, Redox-responsive{,} core-crosslinked degradable micelles for controlled drug release, Polym. Chem. 7 (2016) 6330–6339. https://doi.org/10.1039/C6PY01423B.

[22] J. Davies, A quantitative kinetic theory of emulsion type. I. Physical chemistry of the emulsifying agent. in Gas/Liquid and Liquid/Liquid Interface, in: Proc. Int. Congr. Surf. Act., 1957: pp. 426–438.

[23] A.U. Rehman, M. Collot, A.S. Klymchenko, S. Akram, B. Mustafa, T. Vandamme, N. Anton, Spontaneous nano-emulsification with tailor-made amphiphilic polymers and related monomers, Eur. J. Pharm. Res. 1 (2019) 27–36.

[24] P. Mukerjee, A. Ray, THE EFFECT OF UREA ON MICELLE FORMATION AND HYDROPHOBIC BONDING, J. Phys. Chem. 67 (1963) 190–192. https://doi.org/10.1021/j100795a046.

[25] A.H. Saberi, Y. Fang, D.J. McClements, Fabrication of vitamin E-enriched

nanoemulsions: Factors affecting particle size using spontaneous emulsification, J. Colloid Interface Sci. 391 (2013) 95–102. https://doi.org/https://doi.org/10.1016/j.jcis.2012.08.069.

[26] M.F. Attia, N. Anton, R. Akasov, M. Chiper, E. Markvicheva, T.F. Vandamme, Biodistribution and toxicity of X-ray iodinated contrast agent in nano-emulsions in function of their size, Pharm. Res. 33 (2016) 603–614. https://doi.org/10.1007/s11095-015-1813-0.

[27] N. Anton, T.F. Vandamme, Nano-emulsions and micro-emulsions: Clarifications of the critical differences, Pharm. Res. 28 (2011) 978–985. https://doi.org/10.1007/s11095-010-0309-1.

[28] E. Szwajczak, J. Świergiel, R. Stagraczyński, J. Jadżyn, Viscous and dielectric properties of α-tocopherol and α-tocopherol acetate, Phys. Chem. Liq. 47 (2009) 460–466. https://doi.org/10.1080/00319100902737455.

[29] P. Saulnier, N. Anton, B. Heurtault, J.-P. Benoit, Liquid crystals and emulsions in the formulation of drug carriers, Comptes Rendus Chim. 11 (2008). https://doi.org/10.1016/j.crci.2007.10.005.

[30] N. Anton, J.-P. Benoit, P. Saulnier, Particular conductive behaviors of emulsion phase inverting, J. Drug Deliv. Sci. Technol. 18 (2008). https://doi.org/10.1016/S1773-2247(08)50015-3.

[31] Y. Hong, Z. Li, Z. Gu, Y. Wang, Y. Pang, Structure and emulsification properties of octenyl succinic anhydride starch using acid-hydrolyzed method, Starch - Stärke. 69 (2017) 1600039. https://doi.org/https://doi.org/10.1002/star.201600039.

[32] L. Altuna, M.L. Herrera, M.L. Foresti, Synthesis and characterization of octenyl succinic anhydride modified starches for food applications. A review of recent literature, Food Hydrocoll. 80 (2018) 97–110. https://doi.org/https://doi.org/10.1016/j.foodhyd.2018.01.032.